948–954 Nucleic Acids Research, 1997, Vol. 25, No. 5 © 1997 Oxford University Press

# The structure of 3′-*O*-anthraniloyladenosine, an analogue of the 3′-end of aminoacyl-tRNA

**Barbara Nawrot, Wolfgang Milius[1], Andrzej Ejchart[2], Stefan Limmer and Mathias Sprinzl***

Laboratorium für Biochemie, [1]Laboratorium für Anorganische Chemie and [2]Lehrstuhl für Struktur und Chemie der Biopolymere, Universität Bayreuth, D-95440 Bayreuth, Germany

Received December 5, 1996; Accepted January 20, 1997 NAR-CCDC identifier CCDC-179

## ABSTRACT

**3′-*O*-Anthraniloyladenosine, an analogue of the 3′-terminal aminoacyladenosine residue in aminoacyl-tRNAs, was prepared by chemical synthesis, and its crystal structure was determined. The sugar pucker of 3′-*O*-anthraniloyladenosine is 2′-*endo* resulting in a 3′-axial position of the anthraniloyl residue. The nucleoside is in *syn* conformation, which is stabilized by alternating stacking of adenine and benzoyl residues of the neighboring molecules in the crystal lattice. The conformation of the 5′-hydroxymethylene in 3′-*O*-anthraniloyladenosine is *gauche–gauche*. There are two intramolecular and two intermolecular hydrogen bonds and several H-bridges with surrounding water molecules. The predominant structure of 3′-*O*-anthraniloyladenosine in solution, as determined by NMR spectroscopy, is 2′-*endo*, *gauche–gauche* and *anti* for the sugar ring pucker, the torsion angle around the C4′–C5′ bond and the torsion angle around the C1′–N9 bond, respectively. The 2′-*endo* conformation of the ribose in 2′(3′)-*O*-aminoacyladenosine, which places the adenine and aminoacyl residues in equatorial and axial positions, respectively, could serve as a structural element that is recognized by enzymes that interact with aminoacyl-tRNA or by ribosomes to differentiate between aminoacylated and non-aminoacylated tRNA.**

## INTRODUCTION

The ubiquitous 3′-terminal adenosine of tRNA serves as an acceptor for covalent attachment of the amino acid during enzymatic aminoacylation of tRNA by aminoacyl-tRNA synthetases (1). Several enzymes, protein factors and ribosomes interact with aminoacyl- tRNA or peptidyl-tRNA during protein biosynthesis. In order to avoid inhibition by non-aminoacylated tRNA, these macromolecules have to recognize the aminoacyladenosine on the 3′-end of aminoacyl-tRNA. Indeed, differences in the equilibrium dissociation constants for non-aminoacylated tRNA and aminoacyl-tRNA are, in some cases, up to five orders of magnitude (2). This raises the question about the differences in the structures of aminoacylated and non-aminoacylated tRNA, which provide the structural basis for such efficient discrimination. This problem was addressed by numerous studies (3, and references therein). Experimental methods suitable for detection of gross conformational changes did not indicate a large structural difference in tRNA upon aminoacylation. Methods which specifically probed the structure of the CCA-end of tRNA indicated, however, a change in the conformation and metal binding properties in this part of the molecule upon aminoacylation (3,4). It has not been possible to determine the aminoacyl-tRNA structure by X-ray analysis or NMR spectroscopy. Such investigations are hampered by instability of the aminoacyl ester bond, which is hydrolyzed at ambient temperature and pH 7, with a half-time between 20 and 120 min (5).

The nucleoside antibiotic puromycin resembles the 3′-end of aminoacyl-tRNA. Its structure has been determined by crystallization and X-ray analysis (6), as well as by NMR in solution (7). The amino acid residue in puromycin is, however, linked to adenosine by an amide bond, which may limit the value of this analogue as a structural model for aminoacyl-tRNA. Similarly, the structure of 3′-*O*-acetyladenosine, which has been solved by X-ray crystallography (8), has only limited value as a structural model for 3′-*O*-aminoacyladenosine since it does not possess an α-amino group on the acyl residue.

As determined by NMR spectroscopy, the single-stranded ACCA sequence, which forms the 3′-end of tRNA, is continuously stacked to the RNA helix of the aminoacyl domain (9–11). Fluorescence measurements with tRNA containing a fluorescent adenosine analogue formycin in position 76 revealed that the 3′-end of tRNA in solution has an ordered, stacked structure (12).

The crystal structure of an aminoacyl-tRNA in complex with elongation factor Tu (EF-Tu) and guanosine 5′-(β,γ-imino)-triphosphate has been recently determined (13). In this structure the terminal 3′-adenine 76 of tRNA is not involved in stacking with the penultimate cytosine 75, but instead it is placed in a cleft on the interface between domains I and II of EF-Tu (13). Thus the possibility arises that the destacking of the 3′-terminal adenosine upon aminoacylation is the structural element which determines the recognition of aminoacyl-tRNA by EF-Tu•GTP.

In the present work we investigate the structure of 3′-*O*-anthraniloyladenosine. This compound, which can be chemically synthesized (14), has a structure similar to 3′-*O*-aminoacyladenosine and is sufficiently stable to allow crystallization or NMR studies. It has also been shown that the anthraniloyl group attached to the adenosine 76 of tRNA mimics the structure of aminoacyl-tRNA and allows an efficient interaction of anthraniloyl-tRNA with EF-Tu•GTP (15).

*To whom correspondence should be addressed. Tel: +49 921 552420; Fax: +49 921 552432; Email: mathias.sprinzl@uni-bayreuth.de

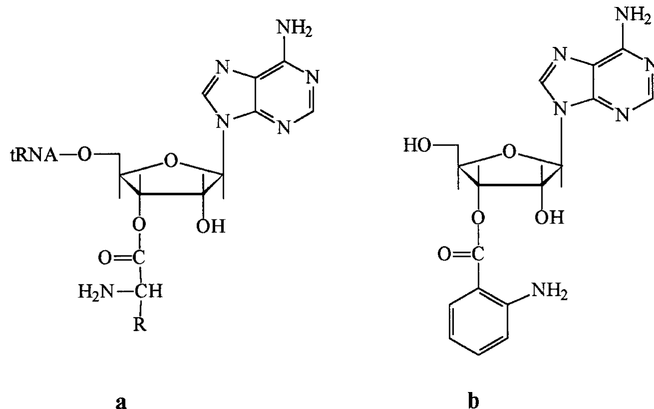


**Figure 1.** Terminal adenosine of 3′-aminoacyl-tRNA. R represents the naturally occurring amino acid side chain (**a**), 3′-*O*-anthraniloyladenosine (**b**).

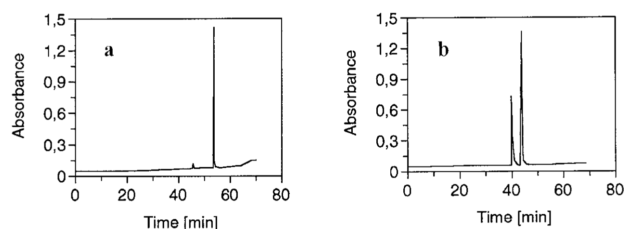


**Figure 2.** HPLC analysis of 2′(3′)-*O*-anthraniloyladenosine and of 2′(3′)-*O*-anthraniloyladenosine at pH 3.5. The peaks at retention times of 45.52 and 53.96 min in (**a**) correspond to 2′- and 3′-*O*-anthraniloyladenosine, respectively. The peaks at retention times 39.89 and 44.46 min in (**b**) correspond to 2′- and 3′-*O*-anthraniloyladenosine 5′-phosphate, respectively.

## MATERIALS AND METHODS

Modification of adenosine with isatoic anhydride was performed according to Hiratsuka (14). Adenosine (1 mmol) was dissolved in 25 ml of water at 38°C. The pH was adjusted to 9.6 with 2 M NaOH, and isatoic anhydride (1.5 mmol) was added to the reaction mixture. The pH was maintained at 9.6 by titration with 2 M NaOH for 2 h. The progress of the reaction was monitored by thin layer chromatography on silica gel plates (Polygram sil $G/UV_{254}$, Roth, Karlsruhe, Germany), in chloroform/methanol, (8:2, v/v). $R_f$ values are 0.38 and 0.73 for adenosine and 2′(3′)-*O*-anthraniloyladenosine, respectively. The reaction mixture was cooled to 0°C, and the product was collected by centrifugation. 3′-*O*-anthraniloyladenosine was isolated from the crude reaction product by crystallization from ethanol/water (1:4, v/v), and purified by silica gel column chromatography (Kieselgel 60, Merck, Darmstadt, Germany) in chloroform/methanol (9:1, v/v). The final purification was achieved by crystallization from ethanol/diethyl ether (5:5, v/v).

HPLC analysis was performed with a Beckman HPLC System Gold using a Supelcosil LC-18S column, 250 × 4.6 mm, with a Supelcosil guard column, (Supelco, Bellafonte, USA). Elution was done at 9°C, with a flow rate of 1 ml/min, with a gradient of 5 mM sodium phosphate buffer pH 3.5 and methanol as follows: 0–5 min, 2.5% methanol; 5–10 min, 10% methanol; 10–65 min, 10–70% methanol gradient; 65–70 min, 70% methanol; 70–80 min: 70–2.5% methanol gradient. Spectrophotometric detection was at 254 and 335 nm. 2′(3′)-*O*-Anthraniloyladenosine 5′-phosphate was obtained under the same conditions as described above, except that after reaction was complete the pH was adjusted to 7.0 with 1 N HCl. The product was isolated from the reaction mixture by chromatography on a Sephadex A-25 column in a 20 mM sodium acetate, pH 5.0, and NaCl gradient from 10 to 250 mM. After desalting on Biogel P6 column the solution was lyophilized to provide pure 2′(3′)-*O*-anthraniloyladenosine 5′-phosphate as a white powder, which was characterized by HPLC, NMR spectroscopy and mass spectrometry.

NOESY NMR spectra were recorded at 500 MHz on a Bruker DRX 500 spectrometer (Bruker, Karlsruhe, Germany) equipped with an Aspect Station computer at 30°C with a mixing time of 200 ms. Adenosine, 3′-*O*-anthraniloyladenosine and 2′(3′)-*O*-anthraniloyladenosine 5′-phosphate were measured as 2 mM solutions in deuterated methanol/$D_2O$ (6:4, v/v) at 23°C. The chemical shifts are given relative to 2,2-dimethyl-2-silapentane-5-sulfonate. Kinetics of 3′- to 2′-transacylation of 3′-*O*-anthraniloyladenosine were measured in phosphate buffer $p^2H$ 7.2/deuterated methanol (87.5:12.5, v/v) at 4°C. The mole fraction of the 2′-*O*-anthraniloyladenosine that was formed was determined by integration of the H1′ peaks in the $^1H$ NMR spectrum. The resulting plot contains data from 128 subsequent spectra; acquisition time for each spectrum was 120 s.

Crystals of 3′-*O*-anthraniloyladenosine for X-ray analysis were grown at 15°C using the sitting drop vapor diffusion method. The 10 µl droplets of 10 mM 3′-*O*-anthraniloyladenosine in ethanol were equilibrated against 1 ml water/ethanol mixtures varying from 9:1 to 3:7 (v/v). For seeding, crystals were transferred to the ethanolic solution of 3′-*O*-anthraniloyladenosine and further equilibrated against water/ethanol 4:6 (v/v).

Intensity data for X-ray structure analysis were collected by Siemens P4 diffractometer with MoKα radiation (λ = 71.073 pm, graphite monochromator). The measurement was carried out at 23°C in the range 3° $\leq 2\theta \leq$ 55° with a scan speed of 2°/min and 1.30° scan range in ω-mode. The intensities of three check reflections, monitored every 100 reflections, were used to control the stability of the primary beam.

The structure of 3-*O*-anthraniloyladenosine was solved by applying Direct Methods (Siemens SHELXTL-PLUS). The refinement was done following the full-matrix-least-squares procedure. All non-hydrogen atoms have been refined with anisotropic temperature factors. The hydrogen atoms involved in H-bridges were found in a difference Fourier synthesis. The remaining hydrogen atoms are in calculated positions. The correct absolute configuration was provided by using a starting material with known configuration.

## RESULTS

### Chemical synthesis

Treatment of adenosine with a 1.5-fold excess of isatoic anhydride at pH 9.6 leads predominantly to formation of a mixture of monosubstituted anthraniloyl-derivatives (Fig. 1). The crude reaction mixture contained 3′-*O*-anthraniloyladenosine (64%), 2′-*O*-anthraniloyladenosine (20%), adenosine (7%), traces of 2′,3′-bis-*O*-anthraniloyladenosine (6%) and isatoic anhydride (3%). Purification by silica gel column chromatography yielded 91% of 3′-*O*-anthraniloyladenosine with a residual 9% contamination by 2′-*O*-anthraniloyladenosine. Crystallization provided 3′-*O*-anthraniloyladenosine (Fig. 2a) contaminated with ~2% 2′-*O*-anthraniloyladenosine.

**Table 1.** Structure determination of 3′-*O*-anthraniloyladenosine; structure solution and refinement

| Crystal data | | Solution and refinement |
|---|---|---|
| Crystal size: 0.20 × 0.15 × 0.12 $mm^3$ | | Number of collected reflections: 2923 |
| Space group: $P2_1$, monoclinic | | Number of unique reflections: 2425 |
| Unit cell dimension: | a = 7.402(2) Å | Final R indices (obs. data): |
| | b = 18.289(2) Å | R = 10.07%, wR = 4.11% |
| | c = 7.670(2) Å | Largest difference peak: 0.43 $eÅ^{-3}$ |
| | β = 113.70(2)° | Largest difference hole: –0.42 $eÅ^{-3}$ |

The 2′(3′)-*O*-anthraniloyladenosine 5′-phosphate was obtained by analogous modification of AMP with isatoic anhydride and isolated from the reaction mixture by ion exchange chromatography. As determined by HPLC of 2′(3′)-*O*-anthraniloyladenosine 5′-phosphate, the equilibrium mixture consisted of 30% 2′-anthraniloyl derivative and 70% 3′-anthraniloyl derivative, giving rise to the peaks at 40 and 44 min, respectively (Fig. 2b). Attempts to purify 3′-*O*-anthraniloyladenosine 5′-phosphate from this mixture by chromatography and crystallization were not successful.

## Crystal structure of 3′-*O*-anthraniloyladenosine

3′-*O*-Anthraniloyladenosine crystallizes as a dihydrate in space group $P2_1$ with two molecules in the asymmetric unit. In this respect 3′-*O*-anthraniloyladenosine exhibits a lower symmetrical crystal structure than puromycin, which crystallizes orthorhombically with space group $P2_12_12_1$ (6). Data pertinent for X-ray structure determination are compiled in Table 1.

The resulting molecular structure of 3′-*O*-anthraniloyladenosine with its atom numbering scheme and solvent molecules is shown in Figure 3a. There are two intramolecular hydrogen bonds: between N3 of purine and the 5′ OH group of ribose and between the carbonyl group and the amino group of the anthraniloyl residue. Two intermolecular hydrogen bonds per molecule are between the amino group of the anthraniloyl residue and the 2′-oxygen atom of the neighboring molecule, and between the amino group of purine and the 2′-oxygen atom of the symmetrically equivalent molecule. Additionally, several hydrogen bonds are possible with surrounding solvent molecules as indicated in Figure 3b. Two intramolecular hydrogen bonds (H5′A-N3 and H11A-O6) influence the stability of the molecule in the adopted conformation. There are no signs of protonation of either N1 of the adenine base or the amino group N11 of the anthraniloyl residue, as is observed for puromycin (6). Amino groups of adenine and anthraniloyl residues have a pyramidal arrangement and consequently their hydrogen atoms are not located on the planes formed by the aromatic system planes. The sugar ring puckering is 2′-*endo* with endocyclic torsion angles $\nu_0$ = –22.2(0.6)°, $\nu_1$ = 35.8(0.5)°, $\nu_2$ = –34.9(0.6)°, $\nu_3$ = 23.3(0.6)°, $\nu_4$ = –0.9(0.6)°. The pseudorotation phase angle P, calculated according to Saenger (16), is 162°, thus in the range of 2′-*endo* ring puckering (144° ≤ P ≤ 180°), whereas the puckering amplitude $\Phi_m$ is 36.4° (17).

The conformation of the 5′-hydroxymethylene group is described by the torsion angle γ O5′–C5′–C4′–C3′ and the alternative torsion angle γ(–) O5′–C5′–C4′–O4′. The values of 49.0(0.8)° and –70.4(0.7)°, respectively, define the conformation around the exocyclic C4′–C5′ bond as *gauche–gauche*.

The glycosidic torsion angle χ(C4–N9–C1′–O4′) of 48.7(0.8)° indicates a *syn* conformation of the nucleoside. This conformation occurs with about the same frequency as the *anti* conformation in the purine nucleosides with a 2′-*endo* sugar pucker. The 3′-*endo* puckering prefers the *anti* orientation around the glycosidic bond (16). The *syn* conformation of 3′-*O*-anthraniloyladenosine is stabilized by an intramolecular hydrogen bond between H5′ and endocyclic nitrogen N3. A similar structure was found for 3′-*O*-acetyladenosine, which crystallizes with 2′-*endo* sugar ring pucker in *syn* conformation of the nucleobase (8) and is stabilized by the same hydrogen bond interaction between 5′ OH and N3 as in the case of 3′-*O*-anthraniloyladenosine. The adenine ring of puromycin and the 3′-terminal adenine in phenylalanyl-$tRNA^{Phe}$ in complex with EF-Tu•GppNHp, adopt an *anti* conformation (6,13).

Both substituents of the phenyl ring in 3′-*O*-anthraniloyladenosine, the carbonyl group and nitrogen atom of the amino group, lie almost in one plane with torsion angles of –4.0(1.0)° and 0.8(0.9)° for O6–C9–C10–C11 and C9–C10–C11–N11, respectively. Additionally, they are in *anti* conformation with respect to the nucleoside part of the molecule. The torsion angle C9–O3′–C3′–C2′ is 168.1(0.5)°. The entire anthraniloyl moiety is slightly twisted out of the C3′–O3′–C9 plane with a torsion angle C3′–O3′–C9–O6 of –2.8(0.9)°.

The aromatic systems of the adenine and the anthraniloyl residue are coplanar, with an angle between the planes of 3.4°, and almost perpendicular to the sugar ring. The angles between the aromatic planes and the sugar ring plane defined by C3′, C4′, O4′ and C1′ atoms are 101.7° and 99.7° for the adenine and anthraniloyl residues, respectively.

In the crystal structure the molecules form parallel layers with a distance of 3.5 Å (Fig. 4). The molecules are arranged similarly in neighboring layers with a translation shift along the y-axis. This arrangement allows strong alternating stacking between the adenine rings and phenyl rings of the adjacent molecules. This stacking of aromatic rings is important for packing of the molecule into the crystal lattice and probably determines the *syn* conformation of the adenine ring. It is known from the X-ray structure of other nucleosides that base stacking plays an important role in stabilization of the base conformation. For example, 4-thiouridine, a naturally-occurring 4-thioketo derivative of uridine, crystallizes from aqueous solution in *syn* conformation. This particular structure is also stabilized by base stacking and hydrogen bonding with surrounding water (18). However, in water solution 4-thiouridine adopts the usual *anti* conformation (19).

## The structure of 3′-*O*-anthraniloyladenosine in solution

The solution structure of 3′-*O*-anthraniloyladenosine was determined by NMR spectroscopy. In aqueous solutions both 2′-*O*-anthraniloyl isomers and 3′-*O*-anthraniloyl isomers exist in equilibrium with the predominant 3′ isomer. This situation is similar to that of the 2′ and 3′ isomers of aminoacyladenosine (20).

In the low field part of the proton NMR spectra (8.27–6.76 p.p.m.) several resonances corresponding to the H2 and H8 protons of the adenosine and protons of the phenyl residue occur. Upfield signals (6.39–3.82 p.p.m.) originate from aliphatic ribose protons. (For full resonance assignments, see ‘Supporting Information’.) In comparison to the unsubstituted adenosine molecule, all anthraniloyl derivatives of adenosine show a downfield shift of ~1 p.p.m. for the ribose proton adjacent to the esterified hydroxyl group. A similar effect, a downfield shift of ~0.3 p.p.m., is observed for

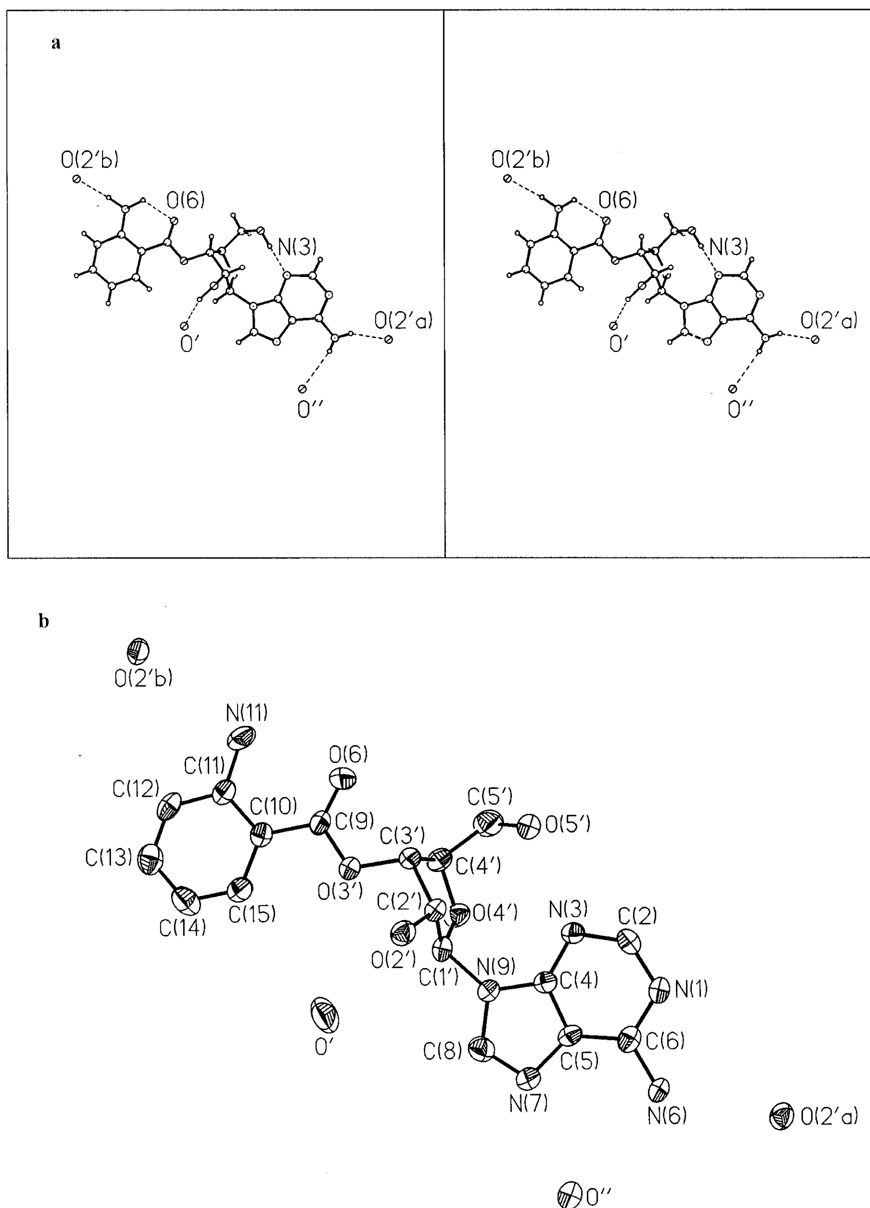


**Figure 3.** Molecular structure of 3′-*O*-anthraniloyladenosine with its atom numbering scheme and solvent molecules (**a**). Stereo view of the molecule with the individual intramolecular and intermolecular hydrogen bonds; oxygen atoms 2′a and 2′b belong to symmetrically equivalent molecules (**b**). The probability level for the thermal ellipsoids is 50%.

neighboring protons (21,22). Resonance signals of 3′-*O*-anthraniloyladenosine are therefore at 5.62 and 5.11 p.p.m. for H3′ and H2′, respectively, whereas corresponding resonances for the adenosine are at 4.40 and 4.77 p.p.m., respectively. Accordingly, in the case of 2′-*O*-anthraniloyladenosine the H1′ proton gives rise to a signal at 6.39 p.p.m., whereas the 3′-*O*-anthraniloyladenosine H1′ proton resonance occurs at 6.16 p.p.m. The relative intensities of both signals reflect the concentration of the isomers. The population ratios of the 2′ isomer to the 3′ isomer, expressed by an equilibrium constant $K_{eq}$, are 0.50 and 0.46 for the 2′(3′)-anthraniloyladenosine and the 2′(3′)-anthraniloyladenosine 5′-phosphate, respectively. The ratio of 2′ isomer to 3′ isomer for several aminoacyladenosine derivatives is, depending on pH and temperature, in the range 0.36–0.47 (21). Thus, as in the case of adenosines esterified with naturally occurring amino acids, 3′-*O*-anthraniloyladenosine is the predominant isomer in an equilibrium mixture under similar conditions.

Furanose ring puckering of 3′-*O*-anthraniloyladenosine was analyzed by vicinal spin–spin coupling constants $^{3}J_{HH}$ (23) (complete compilation of scalar coupling is given in supporting information under Supplementary Material). As was determined for the crystal structure of 3′-*O*-anthraniloyladenosine, the 2′-*endo* conformer is also a predominant conformer in solution. For the corresponding 3′-*O*- anthraniloyladenosine 5′-phosphate, the 2′-*endo* conformer likewise prevails. 2′-*endo* populations of ~78% ($J_{1'2'}$ = 6.4 Hz) for the 2′-*O*-anthraniloyladenosine isomer and 90% ($J_{1'2'}$ = 7.2 Hz) for the 3′-*O*-anthraniloyladenosine isomer can be derived from the scalar coupling constants (23). For 2′-*O*-anthraniloyladenosine 5′-phosphate and 3′-*O*-anthraniloyladenosine 5′-phosphate, the 2′-*endo* populations are 68% ($J_{1'2'}$ =

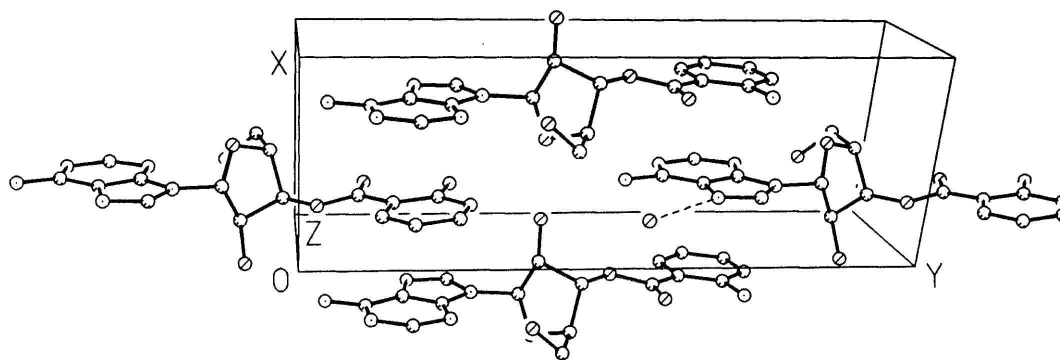


**Figure 4.** Molecular packing of 3′-*O*-anthraniloyladenosine in the crystal lattice with alternating stacks of adenine and anthraniloyl rings.

5.7 Hz) and 90% ($J_{1'2'}$ = 7.2 Hz), respectively. Substitution of a 2′-OH group of adenosine or AMP with the anthraniloyl residue also leads preferentially to the 2′-*endo* conformer, although a decrease in its population by several percent indicates slightly different ring puckering.

The conformation around the C4′–C5′ bond was determined using spin–spin coupling constants $J_{4'5'}$ and $J_{4'5''}$ (see supporting information available as Supplementary Material) (24). The sum of both coupling constants in the range of 5.0 Hz indicates the *gauche–gauche* as the preferred conformer for both 2′- and 3′-*O*-anthraniloyl isomers, ~80% of the population for both isomers.

Determination of the conformation around the glycosidic bond ($\chi$) was performed on the basis of the two-dimensional nuclear Overhauser enhancement spectroscopy. As expected for a low-molecular weight compound, negative cross peaks with respect to the diagonal peaks were observed [positive nuclear Overhauser effect; cf. (25)] The nuclear Overhauser effect cross-peak intensities can be related to the distances between observed proton spins (25). According to the reported intramolecular distances for a canonical A-DNA helix, with the torsion angle in the range of *anti* and pseudorotation angle for the 2′-*endo* conformer, the distances between the base and ribose protons H8–H2′ and H8–H1′ are 3.9 and 3.8 Å, respectively (25). These values determine the relative nuclear Overhauser effect cross-peak intensities to be approximately equal ($I_{H8-H1'}/I_{H8-H2'}$ = 1.17). Similar data analysis for a Z-DNA molecule, which represents *syn* conformation around the glycosidic bond, gives values of 4.1 and 2.3 Å for H8-H2′ and H8-H1′ distances, respectively. The predicted relative magnitude of the NOESY cross-peak intensity ratio should then be on the order of 30. The observed NOESY cross peak pattern involving the ribose protons H1′ and H2′, as well as the H8 proton of the adenine residue, for the mixture of the 2′- and 3′-*O*-anthraniloyladenosine isomers is displayed in Figure 5. The comparison of the relative cross peak intensity ratio for the 3′-*O*-anthraniloyladenosine and 2′-*O*-anthraniloyladenosine gives values of 1.23 and 3.93, respectively. These values indicate a preferred *anti* conformation for both the 2′ isomer and the 3′ isomer. However, the value obtained for the 2′-isomer indicates that a small population of *syn* conformer is in fast exchange with the predominant *anti* conformer. Thus, the relative orientation of the base and the sugar moiety for the anthraniloyl derivatives of adenosine in solution is not determined by alternating stacking of the aromatic systems as observed in the solid state (Fig. 4).

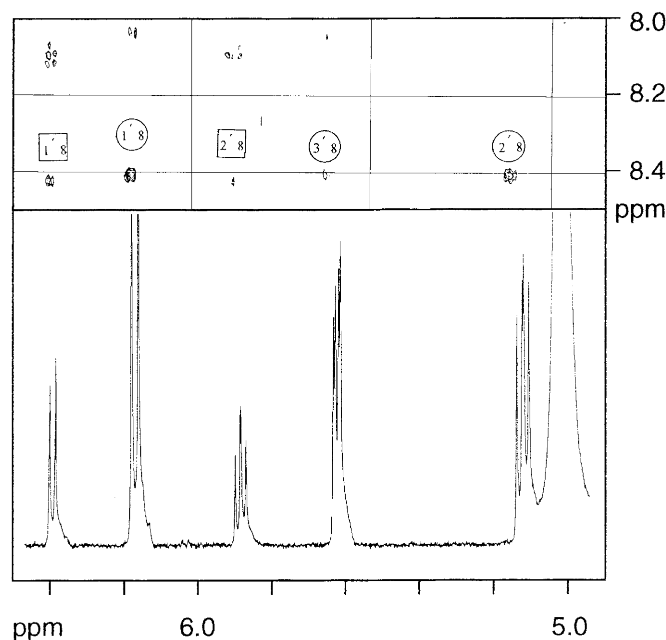


**Figure 5.** The 500 MHz NOESY spectrum of equilibrium mixture of the 3′-*O*-anthraniloyladenosine and the 2′-*O*-anthraniloyladenosine expanded in the region of sugar–base proton interactions. The negative nuclear Overhauser effect cross-peak intensities for 3′-isomer protons are indicated by circles, whereas the ones for the 2′-isomer protons are marked by squares. Below: one-dimensional proton spectrum of 2′(3′)-*O*-anthraniloyladenosine in the range of 6.5–5.0 p.p.m. (deuterated methanol/$D_2O$ 6:4, 23°C).

## Transacylation rate between 2′-*O*-anthraniloyladenosine and 3′-*O*-anthraniloyladenosine

Kinetics of the transacylation reaction between 2′-*O*-anthraniloyl-adenosine and 3′-*O*-anthraniloyladenosine were measured by $^1$H NMR spectroscopy using H1′ peak integrations for mole fraction determination. Equilibrium constant (K), equilibrium rate (k) and transacylation rates ($k_{3'\rightarrow 2'}$ and $k_{2'\rightarrow 3'}$) were determined according to the equation $A(t) = A_e + (A_o - A_e)e^{-kt}$, where $A_o$ and $A_e$ are mole ratios of 2′-*O*-anthraniloyladenosine at time 0 s and at equilibrium, respectively. There, the intensity increase of resonance signals due to the 2′ isomer was analyzed.

**Table 2.** Structural features of crystalline puromycin (6), 3′-*O*-acetyladenosine (8) and 3′-*O*-anthraniloyladenosine

| | 3′-*O*-acetyladenosine | 3′-*O*-anthraniloyladenosine | puromycin |
|---|---|---|---|
| Glycosidic torsion angle (χ) | *syn* | *syn* | *anti* |
| C4′-C5′ bond conformation (γ) | *gauche–gauche* | *gauche–gauche* | *gauche–gauche* |
| Sugar ring pucker | 2′-*endo* | 2′-*endo* | 3′-*endo* |
| Position of C1′-N bond | equatorial | equatorial | axial |
| Position of C3′-O bond | axial | axial | equatorial |

The equilibrium rate $k = k_{3'\rightarrow 2'} + k_{2'\rightarrow 3'}$ (at p$^2$H 7.2 and 4°C) determined in this way was (1.15 × 0.09) x $10^{-4}$ $s^{-1}$, which is almost four orders of magnitude less than the equilibrium rate reported for 2′(3′)-*O*-phenylalanyladenosine [1.01 $s^{-1}$ at p$^2$H 7.3 and 25°C; (21)] The equilibrium constant $K = (k_{3'\rightarrow 2'})/(k_{2'\rightarrow 3'})$, which gives the molar ratio of 2′ and 3′ isomers at equilibrium, amounts to 0.43 ± 0.02, which is very close to the value observed for 2′(3′)-*O*-phenylalanyladenosine [0.40; (21)]. The transacylation rates $k_{3'\rightarrow 2'}$ and $k_{2'\rightarrow 3'}$ are (0.34 × 0.07) × $10^{-4}$ $s^{-1}$ and (0.81 ± 0.04) × $10^{-4}$ $s^{-1}$, respectively. The distinctly slower migration of the anthraniloyl residue as compared to transacylation rates of 2′(3′)-*O*-phenylalanyladenosine (21) is due to the more stable ester bond connecting the anthraniloyl residue with the adenosine moiety and also due to the presence of the aromatic amino function with a pKa 4.95, which is lower than that of the aliphatic α-amino group.

## DISCUSSION

3′-*O*-anthraniloyladenosine is the first aminoacyl derivative of adenosine which was crystallized and its structure determined. Adenosines esterified with proteinogenic amino acids are labile. The ester bond is susceptible to rapid hydrolysis and a transacylation between 2′- and 3′-hydroxyl groups. The presence of the vicinal hydroxyl group is important for both reactions. In one case it accelerates hydrolysis of the ester bond (26), in the other it is the prerequisite for transacylation between the 2′ and 3′ positions. Due to attachment to an aromatic ring, the carboxyl and amino groups of anthranilic acid have a different reactivity as compared to α-amino acids. As a consequence, the rate of hydrolysis and rate of transacylation are more than four orders of magnitude lower than in the case of adenosines esterified with α-amino acids. This allows the study of the structure of 2′(3′)-anthraniloyl-adenosine by crystallography or NMR.

It was reported that anthranilation of adenosine or adenosine 5′-phosphate by isatoic anhydride leads exclusively to 3′-*O*-anthraniloyladenosine derivatives (14). We demonstrate in this work that this is not the case. All available, free hydroxyl groups of adenosine or adenosine 5′-phosphate can be esterified, with preference for the 3′-hydroxyl group. We were successful in isolation of pure 3′-*O*-anthraniloyladenosine, since the structure of this isomer is stabilized by alternative stacking of adenine and phenyl rings in the crystal lattice. This allows the purification of the 3′-isomer by crystallization. We did not succeed, however, in purification of a single isomer of 2′(3′)-*O*-anthraniloyladenosine 5′-phosphate, which could not be prepared in crystalline form.

The crystal structure of 3′-*O*-anthraniloyladenosine has some remarkable features, which are different from the structure of the antibiotic puromycin, but similar to the structure of 3′-*O*-acetyl-adenosine (Table 2). The most significant is the 2′-*endo* pucker of the ribose in the case of the 3′-*O*-anthraniloyl and the 3′-*O*-acetyl derivatives. In contrast, puromycin has a 3′-*endo* conformation both as a crystal (6) as well as in solution (7). We demonstrate in this work that the 2′-*endo* sugar pucker is a predominant conformation for 3′-*O*-anthraniloyladenosine in solution as well. The ribose ring puckering defines the orientation of the glycosidic bond, which is equatorial for the 2′-*endo* conformation, but axial for the 3′-*endo* conformation. This difference may be important for the recognition of the aminoacyl-ated adenosine on the 3′-end of tRNA during various steps in translation. Recently the structure of the EF-Tu in complex with a GTP analogue and aminoacyl-tRNA was determined (13). The terminal adenosine of aminoacyl-tRNA in this structure is not stacked to the penultimate cytosine of the CCA-end, but instead it is extended to a lipophilic pocket of the protein. Since in tRNA that is not aminoacylated, the CCA-end forms a continuous stack (9,10,12), it is possible that aminoacylation of the 3′-terminal ribose causes destacking of adenosine from the CCA-end providing a signal for recognition.

The mechanism leading to this destacking may involve the interaction of the 2′ hydroxyl group of the ribose moiety with the vicinal ester-carbonyl group of the aminoacyl residue. Such an interaction occurs, e.g. during migration of the aminoacyl residue between 2′ and 3′ positions of the terminal adenosine with an obligatory orthoester acid intermediate (27). Correspondingly, it was demonstrated for the interaction of tRNA with aminoacyl-tRNA synthetase that subtle structural variations on the 3′-terminal ribose lead to conformational changes in the tRNA–synthetase complex (28,29). Aminoacylation of tRNA and the presence of a free vicinal OH-group probably lead to structural changes in the CCA-end and formation of 2′-*endo* conformation on the terminal ribose (30).

In A-type RNA the nucleobase is held in axial position, and the ribose adopts the 3′-*endo* conformation. In this case the 3′-substituent is placed to the equatorial position. Such a structure was observed for puromycin, in which the aminoacyl residue, attached by an amide bond to the 3′-position, is equatorial and the ribose possesses a 3′-*endo* conformation. This may be due to the lack of interaction of the amide-carbonyl with the vicinal 2′-hydroxyl group. In agreement with this interpretation aminoacyl-tRNA in which the aminoacyl residue is attached via an amide bond to the 3′ position of the terminal adenosine does not form stable complexes with EF-Tu•GTP (31).

## ACKNOWLEDGEMENTS

This work is dedicated to Professor Max Herberhold on the occasion of his 60th birthday. We would like to thank to Melanie Beikman for help with preparation of the manuscript. The work was supported by the *Deutsche Forschungsgemeinschaft*,

Sp-243/8-1 and the Human Frontier Science Programme, RG-369/93.

**Supplementary data available**

The crystallographic data were deposited at the Cambridge Crystallographic Data Centre as supplementary publication no. CCDC-179. Copies are available, free of charge, on request from: The Director, CCDC, 12 Union Road, GB-Cambridge CB1E2 (fax: +1223 336033).

Tables of the proton chemical shifts and the vicinal scalar coupling constants $^3J_{HH}$ of aminoacylated adenosine derivatives (2′-*O*-anthraniloyladenosine, 3′-*O*-anthraniloyladenosine, 2′-*O*-anthraniloyl-AMP and 3′-*O*-anthraniloyl-AMP) can be found as supporting information for this manuscript (one page). Ordering information is given on any current masthead page.

See supplementary material available in NAR Online.

## REFERENCES

1 Meinnel,T., Mechulam,Y., Lazennec,C., Blanquet,S. and Fayat,G. (1993) *J. Mol. Biol.* **229**, 26–36.
2 Janiak,F., Dell,V.A., Abrahamson,J.K., Watson,B.S., Miller,D.L. and Johnson,A.E. (1990) *Biochemistry* **29**, 4268–4277.
3 Potts,R.O., Ford,N.C.J. and Fournier,M.J. (1981) *Biochemistry* **20**, 1653–1659.
4 Pongs,O., Wrede,P., Erdmann,V.A. and Sprinzl,M. (1976) *Biochem. Biophys. Res. Commun.* **71**, 1025–1033.
5 Schuber,F. and Pinck,M. (1974) *Biochimie*, **56**, 383–390.
6 Sundaralingam,M. and Arora,S.K. (1972) *J. Mol. Biol.* **71**, 49–70.
7 Jardetzky,O. (1963) *J. Am. Chem. Soc.* **85**, 1823–1825.
8 Rao,S.T. and Sundaralingam,M. (1970) *J. Am. Chem. Soc.* **92**, 4963–4970.
9 Limmer,S., Reif,B., Ott,G., Arnold,L. and Sprinzl,M. (1996) *FEBS Lett.* **385**, 15–20.
10 Viani Puglisi,E., Puglisi,J.D., Williamson,J.R. and RajBhandary,U.L. (1994) *Proc. Natl. Acad. Sci. USA*, **91**, 11467–11471.
11 Limmer,S., Hofmann,H.-P., Ott,G. and Sprinzl,M. (1993) *Proc. Natl. Acad. Sci. USA*, **90**, 6199–6202.
12 Maelicke,A., Sprinzl,M., von der Haar,F., Khwaja,T.A. and Cramer,F. (1974) *Eur. J. Biochem.* **43**, 617–625.
13 Nissen,P., Kjeldgaard,M., Thirup,S., Polekhina,G., Reshetnikova,L., Clark,B.F.C. and Nyborg,J. (1995) *Science*, **270**, 1464–1472.
14 Hiratsuka,T. (1983) *Biochim. Biophys. Acta*, **742**, 496–508.
15 Servillo,L., Balestrieri,C., Quagliuolo,L., Iorio,L. and Giovane,A. (1993) *Eur. J. Biochem.* **213**, 583–589.
16 Saenger,W. (1984) *Principles of Nucleic Acid Structure.* Springer-Verlag, New York.
17 Wijmenga,S.S., Mooren,M.M.W. and Hilbers,C.W. (1993) In Roberts,G.C.K. (ed.), *NMR of Macromolecules: A Practical Approach.* IRL Press, Oxford, Vol. I, pp. 217–288.
18 Mazumdar,R. and Saenger,W. (1974) *J. Mol. Biol.* **85**, 213–229.
19 Scheit,K.H. and Saenger,W. (1969) *FEBS Lett.* **2**, 305–308.
20 Taiji,M., Yokoyama,S., Higuchi,S. and Miyazawa,T. (1981) *J. Biochem.* **90**, 885–888.
21 Taiji,M., Yokoyama,S. and Miyazawa,T. (1983) *Biochemistry* **22**, 3220–3225.
22 Griffin,B.E., Jarman,M., Reese,C.B., Sulston,J.E. and Trentham,D.R. (1966) *Biochemistry* **5**, 3638–3649.
23 Altona,C. (1982) *J. R. Netherlands Chem. Soc.*, **101**, 413–433.
24 Davies,D.B. (1978) In Emsley,J.W., Feeney,J. and Sutcliffe,L.M. (eds), *Progress in Nuclear Magnetic Resonance Spectroscopy.* Pergamon Press, New York, Vol 12, pp. 132–225.
25 Wüthrich,K. (1986) *NMR of Proteins and Nucleic Acids.* John Wiley & Sons, New York.
26 Sprinzl,M. and Cramer,F. (1973) *Nature New Biol.*, **245**, 3–5.
27 Chládek,S. and Sprinzl,M. (1985) *Angew. Chem. Int. Ed.* **24**, 371–391.
28 Krauss,G., von der Haar,F. and Maass,G. (1979) *Biochemistry* **18**, 4755–4761.
29 Lefevre,J.F., Bacha,H., Renaud,M., Ehrlich,R., Gangloff,J., von der Haar,F. and Remy,P. (1981) *Eur. J. Biochem.* **117**, 439–437.
30 Potts,R., Fournier,M.J. and Ford,N.C.J. (1977) *Nature*, **268**, 563–564.
31 Sprinzl,M., Kucharzewski,M., Hobbs,J.B. and Cramer,F. (1977) *Eur. J. Biochem.* **78**, 55–61.